



---

*Communication*

## ***Chaetoceros muelleri* sulfated polysaccharides: chain conformation, physical characteristics, and morphology**

**Valeria Miranda-Arizmendi<sup>1</sup>, Jorge Marquez-Escalante<sup>1</sup>, Agustin Rascon-Chu<sup>1</sup>, Karla Martínez-Robinson<sup>1</sup>, Francisco Brown-Bojorquez<sup>2</sup> and Elizabeth Carvajal-Millan<sup>1,\*</sup>**

<sup>1</sup> Research Center for Food and Development (CIAD, AC), Carretera Gustavo Enrique Astiazarán Rosas No. 46, Col. La Victoria, 83304 Hermosillo, Sonora, Mexico

<sup>2</sup> Department of Polymers, University of Sonora, Blvd. Luis Donaldo Colosio, S/N, Hermosillo 83000, Sonora, Mexico

\* **Correspondence:** Email: [ecarvajal@ciad.mx](mailto:ecarvajal@ciad.mx); Tel: +526622892400; Fax: +526622800421.

**Abstract:** Increasing interest in biopolymers moves their knowledge frontiers. One area undergoing this development is polysaccharides. The practical and theoretical significance of studying polysaccharides lies in the numerous essential functions these macromolecules fulfill in living organisms, and the important industrial and technological purposes they serve. Polysaccharides are thought to be abundant in marine microalgae; nevertheless, little is known about their sulfated polysaccharides. We studied *Chaetoceros muelleri* sulfated polysaccharide (CMSP) chain conformation, physical characteristics, and morphology. The CMSP spectrum generated from Fourier-transform infrared analysis displayed distinctive bands for these macromolecules. S=O and C–O–S signals were detected at 1225 and 820  $\text{cm}^{-1}$ , respectively, confirming the presence of sulfate in the molecules. The biopolymer registered weight-average molar mass, intrinsic viscosity ( $[\eta]$ ), radius of gyration (RG), hydrodynamic radius (Rh), and sulfate degree of substitution of 1933 kDa, 577 mL/g, 62 nm, 44 nm, and 0.5 (sulfates per disaccharide repeat unit), respectively. The exponent  $\alpha$  and the coefficient K in the Mark-Houwink-Sakurada (MHS) equation were 0.76 and  $9.76 \times 10^{-3}$  mL/g, respectively. These values suggest a flexible and compact random coil structure in CMSP. The sample's zeta potential ( $\zeta$ ), conductivity, and diffusion coefficient (D) were  $-26.43$  mV,  $-2.07 \mu\text{m cm/s V}$ , 1.25 mS/cm, and  $1.8 \times 10^{-8}$   $\text{cm}^2/\text{s}$ , correspondingly. The negative charge in the molecules is related to the sulfate groups contained. The CMSP surface was coarse and craggy, according to scanning electron microscopy (SEM). The information generated in this present study contributes to elucidating characteristics as fundamental knowledge to understand the macromolecule functionality.

**Keywords:** microalga polysaccharides; macromolecular characterization; multi-angle light scattering; scanning electron microscopy

---

## 1. Introduction

Natural polymers tend to be preferred over synthetic polymers because of their intrinsic properties, such as, biodegradability, biocompatibility, and non-toxicity, which favor their application in the biomedical area [1,2]. Polysaccharides are natural polymers with more than ten monosaccharides linked by glycosidic bonds; some present important functional properties derived from their structural characteristics [3]. Sulfated polysaccharides from marine algae have attracted increasing attention in recent years since they have reported various biological activities, biocompatibility, biodegradability, moisture retention, and colloidal properties [4]. These polysaccharides can be used to develop multiple renewable biomaterials such as drug delivery vehicles, dressings, and others with a biomedical approach [5]. Nevertheless, understanding these macromolecules' functionalities and potential uses requires comprehending their biophysical and microstructural properties.

There are studies regarding the extraction and potential application of sulfated polysaccharides present in marine microalgae from different regions of the world, with the information being less abundant than for marine macroalgae. Due to the intricate processes involved in microalga-sulfated polysaccharide extraction and purification and their chemical structure complexity, only a few structures have been resolved for these macromolecules. Fucose, xylose, galactose, ribose, glucose, mannose, rhamnose, and uronic acids are monosaccharides composing microalga-sulfated polysaccharides [6]. Sulfated polysaccharides present bioactive properties related to their structural characteristics, such as sugar components, molecular weight, and sulfate content. These polysaccharides have been reported to present antitumoral, anticoagulant, antioxidant, and antiviral properties, among others [3,6,7]. The degree of sulfation in marine alga polysaccharides may depend on the algae's genus, species, season, geographic location, and reproductive stage. This sulfate content may affect the polysaccharide bioactivities [8].

Furthermore, because the characteristics of sulfated polysaccharides from algae can vary depending on the growth conditions, different maritime regions may produce differences in the structure and functionality of these biopolymers. We examined the morphology, physical properties, and chain conformation of sulfated polysaccharides derived from the Sea of Cortés microalga *Chaetoceros muelleri*. This maritime region in Northwestern Mexico is also called California Gulf and has been little explored concerning sulfated polysaccharides in microalgae. Additionally, the Sea of Cortés is recognized as an area of global marine conservation significance and has been a protected UNESCO World Heritage Site since 2005 [5]. In this regard, the current research is crucial to developing a thorough scientific understanding of the sulfated polysaccharides in *C. muelleri* growing in the Sea of Cortés.

## 2. Materials and methods

### 2.1. Materials

The sulfated polysaccharide recovered from microalgae *C. muelleri* (CMSP) present in the Sea

of Cortés was extracted as described in a previous study [6,9]. Sigma-Aldrich Chemical Company, located in St. Louis, MO, USA, supplies all chemical reagents.

## 2.2. Fourier transform infra-red (FTIR) spectroscopy

A Nicolet iS50 FT-RI spectrometer (Madison, WI, USA) was used to record the FTIR spectrum of dry CMSP powder. The iS50 ATR analysis was used to analyze the sample. The spectrum was captured between 4000 and 400  $\text{cm}^{-1}$  [9]. The degree of sulfate substitution (DS) in CMSP (sulfates per disaccharide repeat unit) was estimated from the proportion of absorbances at 845 and 2920  $\text{cm}^{-1}$ . The band at 2920 related to C-H stretching serves as a benchmark for the overall amount of sugar, and the band at 845  $\text{cm}^{-1}$  is related to the 3-linked galactose-4-sulfate [10].

## 2.3. Multi-angle light scattering coupled with size exclusion chromatography (SEC-MALS)

Macromolecular characteristics such as weight-average molar mass ( $M_w$ ), number-average molar mass ( $M_n$ ), polydispersity index ( $PI$ ), intrinsic viscosity ( $[\eta]$ ), radius of gyration (RG), hydrodynamic radius (Rh), characteristic ratio ( $C^\infty$ ), persistence length ( $q$ ), and Mark–Houwink–Sakurada constants ( $\alpha$  and  $K$ ) were determined using SEC-MALS. A MALS detector (DAWN HELOS-II 8) coupled with a Viscometer (ViscoStar-II) and a refractive index (Optilab T-rEX) (Wyatt Technology Corp., Santa Barbara, CA, USA) was utilized [9]. A flow rate of 0.7 mL/min (50 mM  $\text{NaNO}_3$ /0.02%  $\text{NaN}_3$  filtered 0.45  $\mu\text{m}$ , Millipore) was applied to an HPLC System (Agilent Technologies, Inc., Santa Clara, CA, USA). The Shodex OH-pak SBH-Q-804 and 805 columns (Shodex Showa Denco K.K., Tokyo, JPN) were used. The ASTRA 6.1 software was applied and developed by Wyatt Technology to analyze and characterize macromolecules. The refractive index increment ( $dn/dc$ ) used was 0.146 mL/g.  $C^\infty$  and  $q$  values were calculated as previously reported [9].

## 2.4. Dynamic light scattering analysis and phase analysis light scattering

Dynamic light scattering (DLS) analysis was applied to investigate zeta potential ( $\zeta$ ), conductivity, and diffusion coefficient ( $D$ ) in CMSP. Furthermore, Phase Analysis Light Scattering (PALS) enabled us to study electrophoretic mobility ( $\mu$ ) [9]. The software DYNAMICS 7.3.1.15 (Wyatt Technology Corp., Santa Barbara, CA, USA) and a Möbiu $\zeta$  (Wyatt Technology Corp., Santa Barbara, CA, USA) were utilized at 25 °C. The sample was dispersed at 0.1% (w/v) using distilled water as the solvent. The Smoluchowski equation was used to calculate electrophoretic mobility with a liquid electric permittivity of 79 and a viscosity of 0.89 cP.

## 2.5. Scanning electron microscopy

CMSP was examined using a 750 $\times$  magnification and a 10 kV voltage in a field emission scanning electron microscope (SEM) (JEOL 5410LV, JEOL, Peabody, MA, USA). Secondary and backscattered electron imaging modes were used to acquire SEM images [6].

### 3. Results

#### 3.1. Fourier transform infra-red (FTIR) spectroscopy

CMSP presented characteristic FTIR absorption bands described regarding sulfated polysaccharides in the literature from marine algae (Figure 1) [10,11]. The signals at 3378 and 2920  $\text{cm}^{-1}$  are associated with the stretching vibration of O–H and C–H links [12]. The 1668–1611  $\text{cm}^{-1}$  bands are attributed to the existence of amide I and amide II groups [9]. The signal at 1388  $\text{cm}^{-1}$  has been related to the C=O group, which may be attributed to carbonyl groups from uronic acids in the molecule. The band at 1102  $\text{cm}^{-1}$  corresponds to the vibrational bond energies of the C–O–C and C–O structures related to glycosidic linkage in polysaccharides [13].

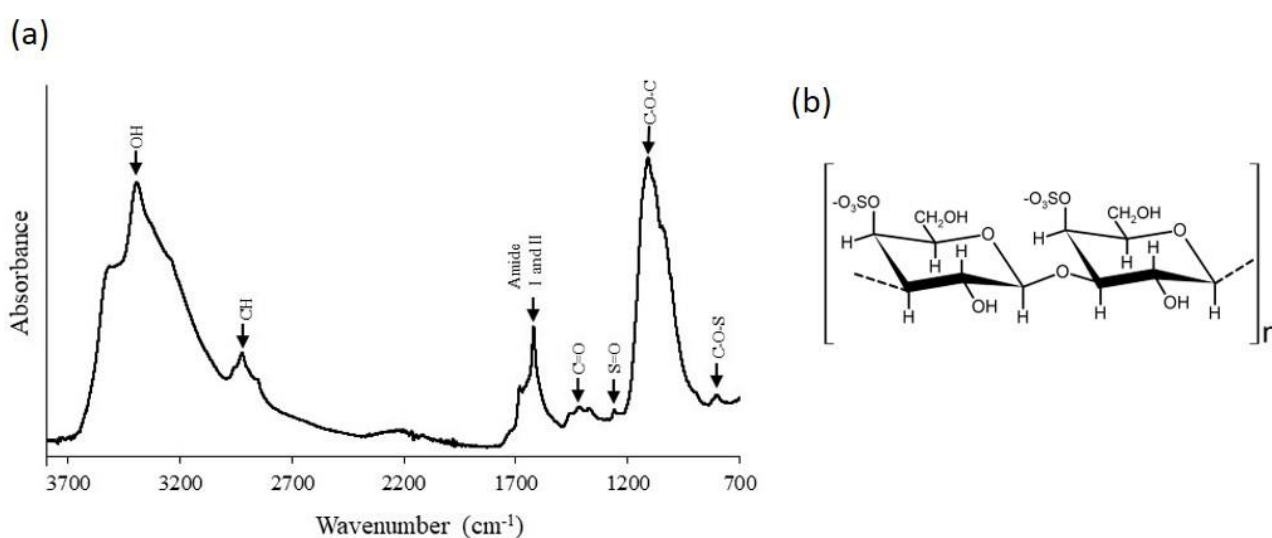


**Figure 1.** (a) FT-IR spectrum of CMSP, (b) Idealized structural segment of CMSP related to 845  $\text{cm}^{-1}$  band, attributed to 3-linked galactose-4-sulfate.

The small band at 1250 and 845  $\text{cm}^{-1}$  indicates the presence of S=O and C–O–S linkages, corresponding to the vibration of the sulfate ester group, confirming sulfate's presence in the polysaccharide. It has been reported that the sulfate content in marine polysaccharides can be estimated from the absorbance ratio at 845/2920  $\text{cm}^{-1}$ . The absorbance at 845  $\text{cm}^{-1}$  has been ascribed to 3-linked galactose-4-sulfate, while the absorbance at 2920  $\text{cm}^{-1}$  associated with C–H has been utilized as an indicator for the total amount of sugar [10]. Based on the ratio of absorbances at 845 and 2920  $\text{cm}^{-1}$ , CMSP's degree of sulfate substitution (DS, sulfates per disaccharide repeat unit) is estimated to be 0.5. Desulfated kappa-carrageenan and sulfated agarose have DS of 0.24 and 0.12, respectively, determined from the 845/2920 absorbances ratio [10]. Knowing the sulfate content and other structural characteristics in polysaccharides, for instance, molecular weight and intrinsic viscosity, is essential to know the relationships between the biopolymers and their potential application [14]. In addition, different sulfate content may modify these polysaccharides' physicochemical properties and bioactivities [15].

### 3.2. Size-exclusion chromatography with multi-angle light scattering

Figure 2 displays the CMSP elution profile along with signals for the light scattering (LS), differential refractive index (dRI), and ultraviolet (UV). A notable peak eluting before minute 10 was part of the sample's bimodal LS response. Small residual proteins may cause the UV signal at high elution times [9]. Table 1 displays the macromolecular properties of CMSP. The radius of gyration (RG), hydrodynamic radius (Rh), intrinsic viscosity [ $\eta$ ], Mw, and polydispersity index (PI) values of CMSP are comparable to those found in the literature for sulfated polysaccharides in marine algae [9,16].

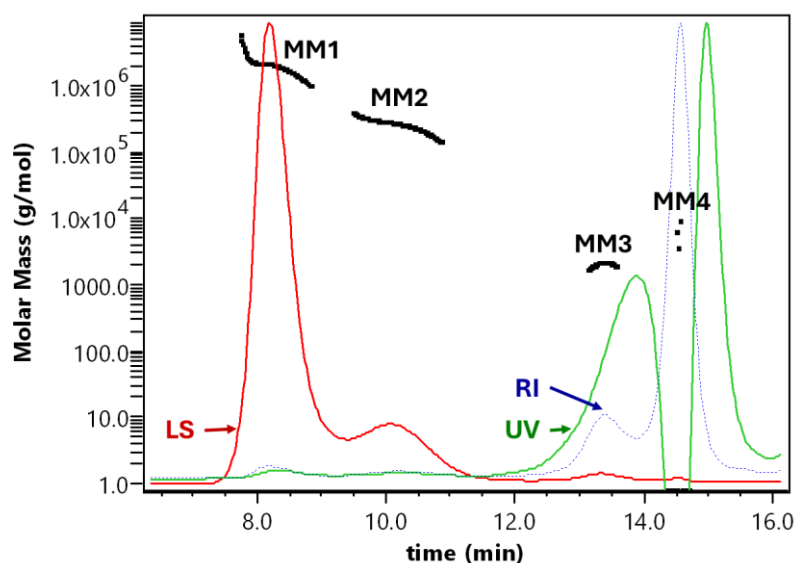


**Figure 2.** SEC-MALS analysis of CMSP. The light scattering (LS), differential refractive index (dRI), and ultraviolet (UV) detector signals, as well as the Molar mass (MM) values, are presented. MM populations 1, 2, 3, and 4 are shown.

K and  $\alpha$  values provide information about the conformation of polysaccharides in the Mark–Houwink–Sakurada equation about intrinsic viscosity. An  $\alpha$  value of 1.26 corresponds to a very rigid chain, while 0.50–0.80 represents flexible random coil structures. Moreover, a low K value denotes a compact coil conformation, and a high K value denotes an expanded coil conformation [17–19]. The  $\alpha$  and K values obtained for CMSP suggest the existence of a flexible and compact random coil structure in these macromolecules.

We computed the  $C_\infty$  and q parameters for the first time. The q value was lower than those reported for macroalga polysaccharides such as alginate [9]. The q value represents the distance over which the chain's direction persists and characterizes the polymer chain flexibility. A lower q value indicates a flexible coil conformation in CMSP.  $C_\infty$  is the ratio of the end-to-end distance of the freely joined chain of n bonds of known length to the observed end-to-end distance of the polysaccharide chain. The  $C_\infty$  value depends on the polysaccharide stiffness; numbers from 7 up to 9 correspond to flexible polymers [17–19]. It is important to note that SEC-MALS yields an average chain conformational space. Nevertheless, structural and conformational elucidation of these macromolecules is necessary for understanding their function. The CMSP conformational characteristics are reported for the first time in this study.

**Table 1.** Macromolecular characteristics of CMSP.

Weight-average molar mass ( $M_w$ , kDa)	1933
Polydispersity index (PI, $M_w/M_n$ )	1.1
Intrinsic viscosity ( $[\eta]$ , mL/g)	577
Radius of gyration (RG, nm)	62
Hydrodynamic radius (Rh, nm)	44
Characteristic ratio ( $C_\infty$ )	7.8
Persistence length (q, nm)	2.2
Mark–Houwink–Sakurada	
Exponent $\alpha$	0.76
Coefficient K	$9.76 \times 10^{-3}$

### 3.3. Physical characteristics

CMSP's physical characteristics are presented in Table 2. In a dispersed macromolecule, the outer region where the ions are less associated has a boundary. The potential in this area is the zeta potential ( $\zeta$ ), and when the macromolecule moves, the ions outside the boundary remain there. CMSP's sulfate content causes the  $\zeta$  potential to be negatively charged. Additionally, a particle's electrophoretic mobility ( $\mu$ ), which is inversely related to conductivity and proportional to the zeta potential (Henry Equation), is represented by its velocity when exposed to an electric field [20]. The diffusion coefficient of CMSP was also determined, representing the fluctuations in scattered light intensity. In this study,  $\zeta$  potential,  $\mu$ , conductivity, and D were higher than those reported for sulfated polysaccharides in *Navicula* sp. [9], possibly due to a high sulfate content in CMSP. These physical characteristics enable a better understanding of macromolecule behavior under aqueous conditions and a possible application in diverse areas, especially those involving biological systems.

**Table 2.** Physical characteristics of CMSP.

Zeta potential ( $\zeta$ , mV)	$-26.43 \pm 3.64$
Electrophoretic mobility ( $\mu$ , $\mu\text{m cm/s V}$ )	$-2.07 \pm 0.28$
Conductivity (mS/cm)	$1.25 \pm 0.01$
Diffusion coefficient (D, $\text{cm}^2/\text{s}$ )	$1.79 \times 10^{-8} \pm 1.14 \times 10^{-9}$

Water as solvent and measurements at 25 °C. The results are expressed as mean  $\pm$  SD.

### 3.4. Scanning electron microscopy (SEM)

CMSP surface microstructure was irregular, with many pores of uneven shape and size (Figure 3). The micrograph suggests repulsive forces between the molecules, resulting in many intermolecular pores, probably related to the negative charge from sulfate groups. The sample also displayed inhomogeneous lumps, suggesting the entanglement and aggregation of CMSP chains. According to a report, a rough surface with some holes could signify the molecule has a branched structure [21]. The CMSP surface morphology generally is similar to that reported for other polysaccharides from marine algae [6–8]. Polysaccharides' surface morphology and interface interactions impact the molecule's functional properties, such as mechanical strength, environmental affinity, and electrostatic interaction.

Additionally, these molecule functionalities define possible applications in medicine, food, and biomaterials.

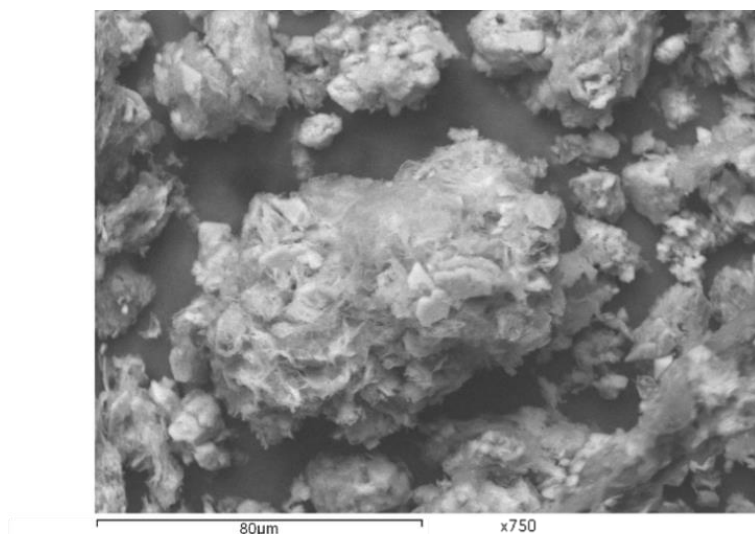


**Figure 3.** Scanning electron microscopy image of CMSP at 750 $\times$  magnification.

#### **4. Conclusions**

We investigated the chain conformation, physical characteristics, and morphology of CMSP. According to the findings, CMSP in an aqueous solution has a compact and flexible random coil conformation and is negatively charged because it contains sulfate. In addition, polysaccharide dispersion presents conductivity and electrophoretic mobility. CMSP surface morphology is rough and forms irregular clusters. This information is essential to predict the CMSP interaction with other molecules and biological systems, which might open the door to new possibilities in applying little-explored marine microalgae sulfated polysaccharides in diverse areas such as biomedicine.

#### **Use of AI tools declaration**

The authors declare they have not used Artificial Intelligence (AI) tools in the creation of this article.

#### **Acknowledgments**

CONAHCYT provided funding for this study under grant number 319684 to E. Carvajal-Millan. Alma C. Campa provided technical support, for which the authors are very grateful.

#### **Conflict of interest**

The authors declare no conflict of interest.

## Author contributions

Conceptualization, E.C.-M. and V.M.-A.; methodology, J.M.-E., V.M.-A., K.G.M.-R. and F.B.-B.; software, J.M.-E., V.M.-A., K.G.M.-R. and F.B.-B.; validation, E.C.-M., J.M.-E. and A.R.-C.; formal analysis, J.M.-E., V.M.-A., K.G.M.-R. and F.B.-B.; investigation, E.C.-M. and V.M.-A.; resources, E.C.-M.; data curation, J.M.-E., V.M.-A., K.G.M.-R., and F.B.-B.; writing—original draft preparation, E.C.-M. and V.M.-A.; writing—review and editing, V.M.-A., J.M.-E., A.R.-C., K.G.M.-R. and F.B.-B.; visualization, E.C.-M. and V.M.-A.; supervision, J.M.-E., A.R.-C. and K.G.M.-R.; project administration, E.C.-M.; funding acquisition, E.C.-M. All authors have read and agreed to the published version of the manuscript.

## References

1. Cai MH, Chen XY, Fu LQ, et al. (2021) Design and development of hybrid hydrogels for biomedical applications: recent trends in anticancer drug delivery and tissue engineering. *Front Bioeng Biotech* 9: 630943. <https://doi.org/10.3389/fbioe.2021.630943>
2. Malafaya PB, Silva GA, Reis RL (2007) Natural–origin polymers as carriers and scaffolds for biomolecules and cell delivery in tissue engineering applications. *Adv Drug Deliver Rev* 59: 207–233. <https://doi.org/10.1016/j.addr.2007.03.012>
3. Kuznetsova TA, Andryukov BG, Besednova NN, et al. (2020) Marine algae polysaccharides as basis for wound dressings, drug delivery, and tissue engineering: a review. *J Mar Sci Eng* 8: 481. <https://doi.org/10.3390/jmse8070481>
4. Tiwari A, Melchor-Martínez EM, Saxena A, et al. (2021) Therapeutic attributes and applied aspects of biological macromolecules (polypeptides, fucoxanthin, sterols, fatty acids, polysaccharides, and polyphenols) from diatoms—a review. *Int J Biol Macromol* 171: 398–413. <https://doi.org/10.1016/j.ijbiomac.2020.12.219>
5. Gilly W, Markaida U, Daniel P, et al. (2022) Long-term hydrographic changes in the gulf of California and ecological impacts: a crack in the world’s aquarium? *Prog Oceanogr* 206: 102857. <https://doi.org/10.1016/j.pocean.2022.102857>
6. Miranda-Arizmendi V, Carvajal-Millan E, Fimbres-Olivarria D, et al. (2022) Macromolecular characteristics of sulfated extracellular polysaccharides from *Chaetoceros muelleri*. Proceedings of the 2nd International Electronic Conference on Diversity (IECD 2022)—New Insights into the Biodiversity of Plants, Animals and Microbes, Basel: Switzerland. <https://doi.org/10.3390/IECD2022-12352>
7. Li S, Zhao Z, He Z, et al. (2024) Effect of structural features on the antitumor activity of plant and microbial polysaccharides: a review. *Food Biosci* 61: 104648. <https://doi.org/10.1016/j.fbio.2024.104648>
8. Ptak SH, Hjuler AL, Ditlevsen SI, et al. (2021) The effect of seasonality and geographic location on sulphated polysaccharides from brown algae. *Aquac Res* 52: 6235–6243. <https://doi.org/10.1111/are.15485>
9. Fimbres-Olivarria D, Marquez-Escalante J, Martínez-Robinson KG, et al. (2023) Physicochemical and microstructural characteristics of sulfated polysaccharide from marine microalga. *Analytica* 4: 527–537. <https://doi.org/10.3390/analytica4040036>



10. Rochas C, Lahaye M, Yaphe W (1986) Sulfate content of carrageenan and agar determined by infrared spectroscopy. *Bot Mar* 29: 335–340. <https://doi.org/10.1515/botm.1986.29.4.335>
11. Miranda-Arizmendi V, Fimbres-Olivarria D, Miranda-Baeza A, et al. (2024) Sulfated polysaccharides from marine diatoms: insight into molecular characteristics and biological activity. *AIMS Bioeng* 11: 110–129. <https://doi.org/10.3934/bioeng.2024007>
12. Liu M, Wang Y, Wang R, et al. (2024) Preparation and performance evaluation of polysaccharide-iron complex of *Eucommia ulmoides*. *Foods* 22: 2302. <https://doi.org/10.3390/foods13142302>
13. Hong T, Yin JY, Nie SP, et al. (2021) Applications of infrared spectroscopy in polysaccharide structural analysis: progress, challenge and perspective. *Food Chem: X* 12: 100168. <https://doi.org/10.1016/j.fochx.2021.100168>
14. Wang Z, Wang L, Yu X, et al. (2024) Effect of polysaccharide addition on food physical properties: a review. *Food Chem* 431: 137099. <https://doi.org/10.1016/j.foodchem.2023.137099>
15. Li S, Zhao Z, He Z, et al. (2024) Effect of structural features on the antitumor activity of plant and microbial polysaccharides: a review. *Food Biosci* 61: 104648. <https://doi.org/10.1016/j.fbio.2024.104648>
16. Yang S, Wan H, Wang R, et al. (2019) Sulfated polysaccharides from *Phaeodactylum tricornutum*: isolation, structural characteristics, and inhibiting HEPG2 growth activity in vitro. *PeerJ* 7: e6409. <https://doi.org/10.7717/peerj.6409>
17. Goh KKT, Pinder DN, Hall CE, et al. (2006) Rheological and light scattering properties of flaxseed polysaccharide aqueous solutions. *Biomacromolecules* 7: 3098–3103. <https://doi.org/10.1021/bm060577u>
18. Picout DR, Ross-Murphy SB, Errington N, et al. (2003) Pressure cell assisted solubilization of xyloglucans: tamarind seed polysaccharide and detarium gum. *Biomacromolecules* 4: 799–807. <https://doi.org/10.1021/bm0257659>
19. Maciel B, Oelschlaeger C, Willenbacher N (2020) Chain flexibility and dynamics of alginate solutions in different solvents. *Colloid Polym Sci* 298: 791–801. <https://doi.org/10.1007/s00396-020-04612-9>
20. Hunter RJ (1981) The calculation of zeta potential, *Zeta Potential in Colloid Science Principles and Applications*, New York: Academic Press, 59–124. <https://doi.org/10.1016/C2013-0-07389-6>
21. Wang Z, Luo D (2023) Extraction optimization, structure features, and bioactivities of two polysaccharides from *Corydalis decumbens*. *Plos One* 18: e0284413. <https://doi.org/10.1371/journal.pone.0284413>



AIMS Press

© 2024 the Author(s), licensee AIMS Press. This is an open access article distributed under the terms of the Creative Commons Attribution License (<http://creativecommons.org/licenses/by/4.0>)